



# COVID-19 Detection on Chest X-ray Images with the Proposed Model Using Artificial Intelligence and Classifiers

Muhammed Yildirim<sup>1</sup> · Orkun Eroğlu<sup>2</sup> · Yeşim Eroğlu<sup>3</sup> · Ahmet Çınar<sup>4</sup> · Emine Cengil<sup>4</sup>

Received: 12 November 2021 / Accepted: 15 April 2022 / Published online: 6 May 2022  
© Ohmsha, Ltd. and Springer Japan KK, part of Springer Nature 2022

## Abstract

Coronavirus disease-2019 (COVID-19) is a serious infectious disease that is spreading rapidly all over the world. Scientists are looking for alternative diagnostic methods to detect and control the disease early. Artificial intelligence applications are promising in the COVID-19 epidemic. This paper proposes a hybrid approach for diagnosing COVID-19 on chest X-ray images and differentiation from other viral pneumonia. The model we propose consists of three steps. In the first step, classification was made using the MobilenetV2, Efficientnetb0, and Darknet53 deep models. In the second step, the feature maps of the images in the Chest X-ray data set were extracted separately for each architecture using the MobilenetV2, Efficientnetb0, and Darknet53 architectures. NCA method was preferred to reduce the size of these feature maps obtained. The feature maps obtained after dimension reduction were classified in the classic machine learning classifiers. In the third step, the feature maps obtained from each architecture were combined. After dimension reduction was applied to these combined features by applying the NCA method, this feature map is classified in the classifiers. The model we proposed was tested on two different data sets. The accuracy values obtained in these data sets are 99.05 and 97.1%, respectively. The obtained accuracy values show that the model is successful.

**Keywords** Artificial Intelligence · Classification · Deep Learning · NCA · X-ray Images

---

✉ Muhammed Yildirim  
muhammed.yildirim@ozal.edu.tr

<sup>1</sup> Department of Computer Engineering, Malatya Turgut Ozal University, Malatya, Turkey

<sup>2</sup> Department of Otorhinolaryngology, Firat University, Elazig, Turkey

<sup>3</sup> Department of Radiology, Firat University, Elazig, Turkey

<sup>4</sup> Department of Computer Engineering, Firat University, Elazig, Turkey

## Introduction

Coronavirus illness 2019 is an infectious disease caused by the severe acute respiratory syndrome coronavirus 2 (SARS-CoV-2) coronavirus, which first appeared in Wuhan, China, in December 2019 [1]. This disease, which is quickly spreading over the globe, has a high morbidity and fatality rate. It is stated that the host of the virus is bats. The coronavirus mainly affects the respiratory system, causing pneumonia. The disease has a wide clinical spectrum, from asymptomatic to fatal. Initial symptoms are fever, weakness, cough, headache, sore throat, and dyspnea may develop in the following days [2]. Finally, it can cause septic shock, acute respiratory distress syndrome, and death, especially in critically ill patients with compromised immune systems and comorbidities [3].

The definitive diagnosis of COVID-19 is realized by a real-time reverse transcriptase-polymerase chain reaction (RT-PCR) test of the throat swab [4]. The main way to control COVID-19 is early diagnosis, rapid isolation, and early treatment. RT-PCR test is the standard method for detecting virus nucleic acid. However, this test may give false-negative results in the early stages of the illness [5]. Furthermore, radiological methods help in the diagnosis and differential diagnosis of the disease. The most significant symptom of the illness is pneumonia in the lungs. The first preferred imaging method is a chest X-ray. In imaging methods, pneumonia foci involving the middle and lower zones of the bilateral lung are seen. However, imaging findings are nonspecific. Similar imaging findings can be seen with various viral pneumonia, such as influenza virus, adenovirus, and cytomegalovirus [6]. Therefore, early diagnosis, rapid isolation, and early treatment are necessary to control COVID-19 [7]. For this reason, it is important to isolate the patient from other viral pneumonia and start the treatment as soon as possible. Artificial intelligence applications are becoming more common in the medical industry. COVID-19 is a serious epidemic disease. In recent years artificial intelligence applications have been used in areas, such as the diagnosis of COVID-19, the prediction of its epidemiological course, and the determination of treatment methods. With artificial intelligence applications, early diagnosis of this disease can be provided, reducing the workload of health workers and supporting health services. It can also contribute to global crisis management when the patient population increases. In addition, it can reduce the economic damage of the epidemic. This study aims to diagnose COVID-19 and differentiate it from other viral pneumonia using artificial intelligence methods on chest X-ray images. In the study, we have used two data sets of chest X-rays of three classes: normal, COVID-19, and viral pneumonia [8].

## Literature Review

There are many studies in the literature on COVID-19. In their study, Maghdid et al. [9] used chest X-ray images and computed tomography (CT) images to classify COVID-19 disease. As a method, they preferred CNN architectures. The

Alexnet model is the preferred model by the authors. In this study, they achieved an accuracy rate of 94.1% with pre-trained CNN architectures.

Yildirim et al. used a three-class data set consisting of chest X-ray images in their study. COVID-19, normal, and pneumonia X-ray images are used in this paper. The authors proposed a new model using the resnet50 architecture as a base in their study. In this paper, an accuracy rate of 96.30% was obtained [10].

Asnaoui et al. examined the COVID-19 disease in their study. They used five pre-trained CNN architectures to classify the images in the data set of chest images. They stated that the accuracy rate they obtained in the Inception-ResNetV2 architecture was 92.18% [11].

Baltruschat et al. used Resnet38, Resnet50, and Resnet101 architectures to classify chest X-ray images in their research. The authors stated that Resnet38 was more successful in this study. In addition, it was seen that class activation charts were used to understand the classification process in the study. In this study, the joint accuracy value was 82.2% [12].

Farid et al. used chest CT and X-ray images in their study. As a result, 98.20% accuracy rate was get in the proposed CNN approach. In the proposed model, using feature extraction methods, the obtained features are classified in machine learning Classifiers [13].

Aslan et al. proposed two different methods for the classification process in their study. In the study, the authors proposed a hybrid model using CNN and LSTM structures. While the accuracy rate in the first model they suggested was 98.14%, the second model's accuracy rate was 98.70% [14].

To detect COVID-19 infection in chest X-ray images automatically, Khan et al. introduced Coronet, a deep CNN model based on the Xception architecture. They got an overall accuracy rating of 89.6 percent with their model [15].

Bai et al. used LSTM and Multilayer perceptions together in their proposed approach. They stated that the model they proposed in this classification was successful. The accuracy rate they obtained in the proposed approach is 89.1% [16].

Mahmud et al. proposed a deep CNN model, called CovXNet, to distinguish between COVID-19 and other types of pneumonia in chest images. This model discriminated COVID-19 from normal chest X-ray with an accuracy rate of 97.4% and COVID-19 from viral pneumonia with 96.9% accuracy [17].

Ucar et al. diagnosed COVID-19 with a 98.3% accuracy rate on chest X-ray images using the SqueezeNet model by adding Bayesian optimization [18].

Minaee et al. proposed the DenseNet-121, Resnet50, ResNet18, and Squeezenet models to detect COVID-19 in chest X-rays. Researchers stated that they obtained approximately 90% specificity and 98% sensitivity with this model [19].

Barua et al. used 3 different CNN architectures for feature extraction in their study. In this study, AlexNet, VGG16 and VGG19 architectures feature maps obtained from the fully connected layer are combined. These feature maps were then classified in the SVM classifier. In the study, accuracy values of 97.60, 89.96, 98.84 and 99.64% were obtained, respectively [20].

## Contributions and Novelty

The COVID-19 epidemic continues widely around the world. Examination of COVID-19 data by an expert is of great importance in terms of time and cost. In this study, we developed a CNN-based hybrid model to diagnose and classify COVID-19 images. In the proposed model, the current models that are frequently used in the literature are used as the base. In our proposed model, the different features of COVID-19 images were obtained using Mobilenetv2, Efficientnetb0 and Darknet53 models as a base. These features were then concatenated. Finally, NCA dimension reduction method was used to make our model run faster and produce more accurate results. Feature maps optimized by NCA method were classified into six different machine learning classifiers. The proposed model has been tested on two different data sets. The accuracy values obtained in these data sets are 99.05 and 97.1%, respectively. The obtained accuracy value showed that the proposed model can successfully classify COVID-19 images.

## Organization of Paper

In the first section of the study, information about COVID-19 and literature research are given. In the second part, the data sets used in the study, the methods used, and the suggested steps are examined. Then we evaluated the obtained application results. Finally, we have completed the study with the discussion and conclusion section.

## Materials and Methods

This section examines the data set, deep models, classifiers, the NCA size reduction method, and the proposed approach that we use in the study.

### Data Sets

In this study, we have used two different data sets. There are three types of classes in these data sets. These classes consist of COVID-19, normal and viral pneumonia chest X-ray images. Required data sets are freely available to the public on the Kaggle website [8]. The first data set has 137 COVID-19, 90 viral pneumonia and 90 normal chest X-ray images, other data set has 3616 COVID-19, 1345 viral pneumonia and 10,192 normal chest X-ray images [21, 22]. Sample images from the data sets are presented in (Fig. 1).

### Deep Models, Classifiers and NCA Method

Deep learning architectures have been widely used in the classification of biomedical images in recent years [23–25]. In this study, the results were obtained using Alexnet, Resnet50, Googlenet, VGG16, Densenet201, Efficientnetb0, Darknet53,

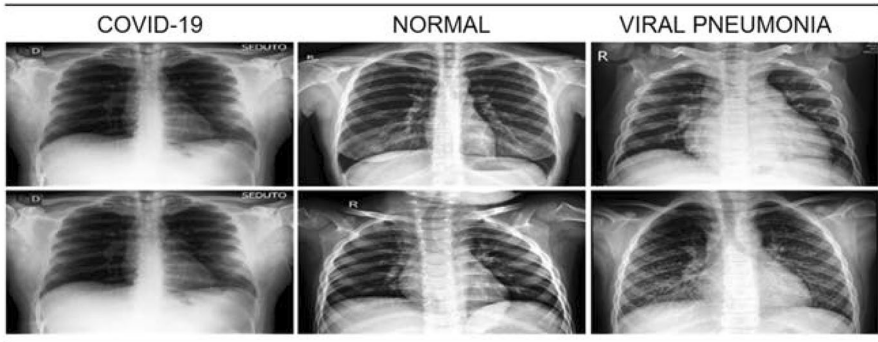


**Fig. 1** Examples of chest X-ray images

Shufflenet, and InceptionV3 models. However, in our proposed model, Darknet53, MobilenetV2 and Efficientnetb0 architectures are used as the base. YOLOv3 is a convolutional neural network used in the object detection approach. It has been developed by making improvements in Darknet19. Unlike Darknet53, the more layers are now used in addition to connections. It has a deeper structure than Darknet19 [26].

Another deep learning model we have used in the study is MobilenetV2. Due to the fact that increasing number of large data sets, the processing power of the models is increasing, and the models are becoming more complex. Therefore, the need for models with fewer parameters, high performance, and working speed is increasing. The Mobilenet architecture is a model developed with this logic in Howard et al. [27]. The Mobilenet architecture is designed for mobile applications and deep learning studies. Various updates were made to the MobilenetV2 model in 2019. In this model, the size of feature maps is reduced using  $1 \times 1$  convolutions [28].

The last deep learning model we have used in the study is Efficientnet. The Efficientnet model is a model developed by the GoogleBrain team. This model is not developed solely based on the depth of the network. In this model, width, resolution, and depth were used together. It has been stated that the width and resolution are effective in the performance of the models. Network width scaling is commonly preferred for small-size models. This is why larger networks can capture more detailed features and are easier to train. However, extensive but shallow networks tend to have difficulty capturing higher level features [29].

The data set was classified with deep learning architectures in this study, and feature maps were obtained using these architectures. NCA method was used to reduce the size of the obtained feature maps. One of the most basic methods used to reduce the size of increasing data amounts is feature selection [30]. NCA method is also a method used for feature selection. The reduced size feature maps were classified in classifiers. In the proposed method, the maximum accuracy value was achieved.

It is known that SVM is a technique used to logically separate data belonging to more than one class from each other in the most appropriate way [31]. For this, decision boundaries or, in other words, hyperplanes are determined. SVM can produce

successful results in high-dimensional spaces. In addition, SVM uses memory efficiently thanks to the training points it uses [32].

## Proposed Approach

The study was performed to classify the images in the data set consisting of chest X-ray images as COVID-19, normal, and, viral pneumonia. In the first step, the images were classified using the pre-trained deep learning architectures.

In the second step of the study, feature maps of chest X-ray images in the data set were obtained using deep architectures. NCA dimension reduction method was applied to the feature maps obtained in each architecture. Then, the new feature maps obtained were classified in the machine learning classifiers [33].

In the third step of the study, the feature maps obtained from the Resnet50, MobilenetV2, and Efficientnetb0 models were concatenated. The size of the feature maps obtained in each architecture was  $317 \times 1000$ , while the size of the feature map after merging was  $317 \times 3000$ . Then, the NCA optimization algorithm was used to save time and cost. As a result, the size of the optimized feature map was  $317 \times 82$ . In other words, out of 3000 features, the best 82 were chosen. The remaining features were eliminated. Finally, these feature maps were classified into different classifiers. The suggested approach is given in (Fig. 2).

## Experimental Results

The research was implemented in a Matlab environment. The Computer used has an i5 processor, 16 GB of RAM, and an 8 GB graphics card. Parameter values are fixed in the model and classifiers. Thus, the same parameter values are used in different architectures and different classifiers. In the study, first, we obtained results from pre-trained models. Then, using the same deep models, the feature maps of the images in the data set were extracted, optimized with NCA, and then classified in classical machine learning classifiers. In the last stage, the proposed method is detailed. In the study, Sensitivity, Accuracy, Specificity, F-measure, FPR, FDR, and FNR parameters [34] were used to measure the performance values metric of the models.

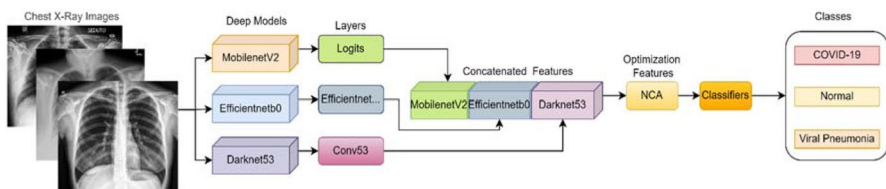


Fig. 2 Proposed Approach

**Table 1** Training parameters

Environment	Max_Epochs	Mini Batch Size	Learning Rate	Optimization
Matlab 2021b	5	16	1e-4	Sgdm

**Table 2** Accuracy rate of pre-trained architectures

Efficientnetb0	MobilenetV2	Darknet53	Alexnet	Resnet50	Densenet201	Googlenet	InceptionV3
77.7%	88.8%	92.06%	93.65%	93.65%	92.06%	90.48%	79.37%

## Pre-trained Deep Architectures

In the first step of the study, the results were obtained using three deep learning architectures. These deep learning models are pre-trained. The same training parameters were used in these three architectures. In addition, we studied on the original data set. Data multiplexing methods were not used to show the performance of the proposed approach. While 20% of the data was reserved for testing, 80% was used for training the model [35]. The training parameters used in the paper are given in (Table 1).

The study was conducted in Matlab 2021b environment. In this study, the epoch value was taken as 5. LearnRate value is 1e-4, minibatch size value is 16 depending on computer memory, and Sgdm is used as optimizer.

The accuracies of the pre-trained models are presented in (Table 2).

The highest accuracy values were obtained in the pre-trained deep models in Alexnet and Resnet50 architectures with 93.65%. Densenet201 and Darknet53 architectures followed this with 92.06%, respectively. The lowest accuracy value was obtained in Efficientnetb0 architecture with 77.7%. The accuracy value obtained in MobilenetV2 was 88.8%, the accuracy value obtained in Googlenet architecture was 90.48%, and the accuracy value obtained in InceptionV3 architecture was 79.37%. Confusion matrixes obtained with pre-trained deep models are shown in (Table 3).

When (Table 3) is analyzed, it is seen that the most successful models are Alexnet and Resnet50. Alexnet and Resnet50 architectures classified 59 of 63 X-ray test images correctly, while 4 of them were misclassified. The Alexnet architecture correctly predicted all 27 COVID-19 and 18 Viral Pneumonia images. Alexnet architecture correctly predicted 14 of the 18 normal X-ray images and incorrectly predicted 4 of them. Resnet50 architecture correctly predicted all 27 COVID-19 X-ray images. Of the two images he mispredicted, two of them actually belonged to the class of normal, while he mispredicted as viral pneumonia. Similarly, the Resnet50 model incorrectly predicted two viral pneumonia images as Normal X-ray images. The lowest accuracy value was obtained in the Efficientnetb0 architecture using pre-trained deep models in the classification process. Of the 63 chest X-ray test images, the Efficientnetb0 architecture predicted 49 correctly and incorrectly predicted 14. When the results obtained using pre-trained deep models in our study are examined,

**Table 3** Confusion matrices for pre-trained models

	Efficientnetb0	MobilenetV2	Darknet53	Alexnet																																																
1	<table border="1"><tr><td>26</td><td></td><td>1</td></tr><tr><td></td><td>13</td><td>5</td></tr><tr><td>4</td><td>4</td><td>10</td></tr><tr><td>1</td><td>2</td><td>3</td></tr></table>	26		1		13	5	4	4	10	1	2	3	<table border="1"><tr><td>27</td><td></td><td></td></tr><tr><td></td><td>12</td><td>6</td></tr><tr><td>1</td><td></td><td>17</td></tr><tr><td>1</td><td>2</td><td>3</td></tr></table>	27				12	6	1		17	1	2	3	<table border="1"><tr><td>27</td><td></td><td></td></tr><tr><td></td><td>13</td><td>5</td></tr><tr><td></td><td></td><td>18</td></tr><tr><td>1</td><td>2</td><td>3</td></tr></table>	27				13	5			18	1	2	3	<table border="1"><tr><td>27</td><td></td><td></td></tr><tr><td></td><td>14</td><td>4</td></tr><tr><td></td><td></td><td>18</td></tr><tr><td>1</td><td>2</td><td>3</td></tr></table>	27				14	4			18	1	2	3
26		1																																																		
	13	5																																																		
4	4	10																																																		
1	2	3																																																		
27																																																				
	12	6																																																		
1		17																																																		
1	2	3																																																		
27																																																				
	13	5																																																		
		18																																																		
1	2	3																																																		
27																																																				
	14	4																																																		
		18																																																		
1	2	3																																																		
	Resnet50	Densenet201	Googlenet	InceptionV3																																																
1	<table border="1"><tr><td>27</td><td></td><td></td></tr><tr><td></td><td>16</td><td>2</td></tr><tr><td></td><td>2</td><td>16</td></tr><tr><td>1</td><td>2</td><td>3</td></tr></table>	27				16	2		2	16	1	2	3	<table border="1"><tr><td>26</td><td></td><td>1</td></tr><tr><td></td><td>15</td><td>3</td></tr><tr><td>1</td><td></td><td>17</td></tr><tr><td>1</td><td>2</td><td>3</td></tr></table>	26		1		15	3	1		17	1	2	3	<table border="1"><tr><td>27</td><td></td><td></td></tr><tr><td></td><td>12</td><td>6</td></tr><tr><td></td><td></td><td>18</td></tr><tr><td>1</td><td>2</td><td>3</td></tr></table>	27				12	6			18	1	2	3	<table border="1"><tr><td>27</td><td></td><td></td></tr><tr><td>1</td><td>6</td><td>11</td></tr><tr><td>1</td><td></td><td>17</td></tr><tr><td>1</td><td>2</td><td>3</td></tr></table>	27			1	6	11	1		17	1	2	3
27																																																				
	16	2																																																		
	2	16																																																		
1	2	3																																																		
26		1																																																		
	15	3																																																		
1		17																																																		
1	2	3																																																		
27																																																				
	12	6																																																		
		18																																																		
1	2	3																																																		
27																																																				
1	6	11																																																		
1		17																																																		
1	2	3																																																		

it is seen that the results obtained in each architecture differ from each other. Therefore, it is obvious that the performance of deep models is closely related to the data set.

### Deep Models + NCA + Classifiers

In the second step of the study, we obtained the feature maps of the images using the deep models. The size of the feature map obtained in each architecture is  $317 \times 1000$ . We applied the NCA dimension reduction method to the feature map obtained in each architecture separately. In the NCA technique, default parameter values are utilized to pick features. To estimate the feature weights, Stochastic Gradient Descent was chosen as the solvent. The study’s Verbosity Level Indicator rating is 1. After applying the NCA method to the feature maps, the size of the new feature maps are given in (Table 4).

The average accuracy values obtained when the feature maps in (Table 4), which were obtained after applying the NCA method to the feature maps we obtained using deep models, were classified in various classifiers, are presented in (Table 5). The k-fold value was chosen as five when the new feature maps obtained after the NCA process was applied to the feature maps obtained in these deep models.

When (Table 5) is examined, the highest accuracy value with an average of 97.47% was obtained by classifying the feature maps obtained using the Darknet53 architecture in the KNN classifier after NCA processing. The Darknet53 architecture was followed by Efficientnetb0+NCA+SE with an average accuracy of 97.16%,

**Table 4** New dimensions of feature maps obtained after applying NCA to feature maps

Efficient-netb0	Mobile-netV2	Darknet53	Alexnet	Resnet50	Densenet201	Googlenet	InceptionV3
$1000 \times 127$	$1000 \times 120$	$1000 \times 137$	$1000 \times 91$	$1000 \times 120$	$1000 \times 65$	$1000 \times 135$	$1000 \times 40$

**Table 5** Feature maps, NCA, classifiers

Deep Models	Accuracy Value of Classifiers(Mean % ± Standard Deviation)					
	DT	DA	NB	SVM	KNN	SE
Resnet50	87.00 ± 3.70	93.05 ± 1.11	94.55 ± 0.33	<b>96.21 ± 0.67</b>	95.67 ± 0.15	96.02 ± 1.58
InceptionV3	76.80 ± 0.96	<b>91.48 ± 0.34</b>	88.50 ± 0.84	88.10 ± 0.62	89.16 ± 1.53	89.63 ± 1.62
Darknet53	84.07 ± 1.29	93.92 ± 0.56	95.02 ± 0.67	96.45 ± 1.19	<b>97.47 ± 0.17</b>	97.27 ± 0.02
MobilenetV2	81.22 ± 2.20	<b>96.52 ± 1.41</b>	94.95 ± 0.78	95.22 ± 0.28	95.20 ± 0.42	95.42 ± 0.80
Alexnet 90	82.97 ± 2.85	92.27 ± 0.56	92.86 ± 0.88	94.57 ± 0.75	<b>94.63 ± 0.61</b>	94.40 ± 1.12
Densenet201	83.57 ± 2.77	93.92 ± 1.23	94.32 ± 0.42	94.37 ± 0.28	<b>95.89 ± 1.38</b>	95.10 ± 0.62
Googlenet	81.77 ± 1.93	88.25 ± 2.24	91.72 ± 0.37	91.57 ± 0.28	93.18 ± 1.37	<b>93.37 ± 1.04</b>
Efficientnetb0	83.17 ± 3.18	94.82 ± 1.04	95.67 ± 0.37	96.6 ± 0.66	96.85 ± 0.42	<b>97.16 ± 0.35</b>

The significance of bold values are indicate high values in the rows

respectively. The third successful hybrid model was Resnet50 + NCA + SVM, with an average accuracy of 96.21%. In the proposed hybrid model, these three models with the highest accuracy value were used as the base. After applying NCA to the feature maps obtained in the models, the obtained feature maps were classified into six different machine learning classifiers. Confusion matrices obtained according to the highest average accuracy values obtained by these deep models in the classifiers, where they are the most successful are given in (Table 6).

After applying the NCA dimension reduction method to the feature map we obtained in the Darknet53 architecture, which we used as the base in the study, it obtained the highest accuracy value among other deep models with an average accuracy value of 97.47%. While classifying the feature maps obtained in the Darknet53 model, the most successful classifier was KNN. When the feature maps obtained in the Darknet53 architecture were classified in the KNN classifier after size reduction,

**Table 6** Deep models + NCA + classifiers

Resnet50 + NCA +	InceptionV3 + NCA +	Darknet53 + NCA +	MobilenetV2 + NCA +																																																
SVM	DA	KNN	DA																																																
1 <table border="1"><tr><td>133</td><td>2</td><td>2</td></tr><tr><td>1</td><td>87</td><td>2</td></tr><tr><td></td><td>5</td><td>85</td></tr><tr><td>1</td><td>2</td><td>3</td></tr></table>	133	2	2	1	87	2		5	85	1	2	3	1 <table border="1"><tr><td>134</td><td>2</td><td>1</td></tr><tr><td>2</td><td>75</td><td>13</td></tr><tr><td></td><td>9</td><td>81</td></tr><tr><td>1</td><td>2</td><td>3</td></tr></table>	134	2	1	2	75	13		9	81	1	2	3	1 <table border="1"><tr><td>134</td><td>2</td><td>1</td></tr><tr><td>1</td><td>88</td><td>1</td></tr><tr><td>2</td><td>1</td><td>87</td></tr><tr><td>1</td><td>2</td><td>3</td></tr></table>	134	2	1	1	88	1	2	1	87	1	2	3	1 <table border="1"><tr><td>134</td><td></td><td>3</td></tr><tr><td>1</td><td>88</td><td>1</td></tr><tr><td></td><td>6</td><td>84</td></tr><tr><td>1</td><td>2</td><td>3</td></tr></table>	134		3	1	88	1		6	84	1	2	3
133	2	2																																																	
1	87	2																																																	
	5	85																																																	
1	2	3																																																	
134	2	1																																																	
2	75	13																																																	
	9	81																																																	
1	2	3																																																	
134	2	1																																																	
1	88	1																																																	
2	1	87																																																	
1	2	3																																																	
134		3																																																	
1	88	1																																																	
	6	84																																																	
1	2	3																																																	
Alexnet + NCA +	Densenet201 + NCA +	Googlenet + NCA +	Efficientnetb0 + NCA +																																																
KNN	KNN	SE	SE																																																
1 <table border="1"><tr><td>134</td><td>2</td><td>1</td></tr><tr><td>1</td><td>86</td><td>3</td></tr><tr><td>2</td><td>8</td><td>80</td></tr><tr><td>1</td><td>2</td><td>3</td></tr></table>	134	2	1	1	86	3	2	8	80	1	2	3	1 <table border="1"><tr><td>133</td><td>3</td><td>1</td></tr><tr><td>1</td><td>88</td><td>1</td></tr><tr><td></td><td>6</td><td>84</td></tr><tr><td>1</td><td>2</td><td>3</td></tr></table>	133	3	1	1	88	1		6	84	1	2	3	1 <table border="1"><tr><td>133</td><td></td><td>4</td></tr><tr><td></td><td>84</td><td>6</td></tr><tr><td></td><td>11</td><td>79</td></tr><tr><td>1</td><td>2</td><td>3</td></tr></table>	133		4		84	6		11	79	1	2	3	1 <table border="1"><tr><td>135</td><td></td><td>2</td></tr><tr><td>1</td><td>89</td><td></td></tr><tr><td></td><td>6</td><td>84</td></tr><tr><td>1</td><td>2</td><td>3</td></tr></table>	135		2	1	89			6	84	1	2	3
134	2	1																																																	
1	86	3																																																	
2	8	80																																																	
1	2	3																																																	
133	3	1																																																	
1	88	1																																																	
	6	84																																																	
1	2	3																																																	
133		4																																																	
	84	6																																																	
	11	79																																																	
1	2	3																																																	
135		2																																																	
1	89																																																		
	6	84																																																	
1	2	3																																																	

**Table 7** Proposed model's accuracy rates

	Accuracy Rate of Proposed Models (Mean % $\pm$ Standard Deviation)					
	DT	DA	NB	SVM	KNN	SE
Proposed Model	83.92 $\pm$ 1.13	95.84 $\pm$ 1.36	97.54 $\pm$ 0.48	<b>99.05 <math>\pm</math> 0.31</b>	98.42 $\pm$ 0.45	98.10 $\pm$ 0.62

The significance of bold values are indicate high values in the rows

**Table 8** Confusion matrices in the three classifiers, where the model is most successful

	Proposed + SVM			Proposed + KNN			Proposed + SE		
1	136		1	135	1	1	136		1
2		89	1		89	1		89	1
3		1	89		2	88		3	87
	1	2	3	1	2	3	1	2	3

the KNN classifier correctly classified 309 chest X-ray images out of 317 and misclassified 8 of them. In the paper, feature maps were created using 8 different models. These extracted feature maps were classified into six different classical machine learning classifiers after dimension reduction. As shown in (Table 6), the classifiers in which each deep model reaches the highest accuracy value are different. While the Resnet50 architecture achieved the highest accuracy in the SVM classifier, the InceptionV3 and MobilenetV2 DA classifiers, the Darknet53, Alexnet, and Densenet201 architectures in the KNN classifier, and the Googlenet and Efficientnetb0 architectures achieved the highest accuracy in the SE classifier.

### The Results Obtained in the First Data Set with the Proposed Method

In this section, the features acquired from the three deep learning models used in the study were combined. The deep models used as the base in the study are MobilenetV2, Efficientnet B0 and Darknet53 models. While the size of the feature map obtained in each model was  $317 \times 1000$ , the size obtained after merging was  $317 \times 3000$ . Size reduction was made by applying the NCA method to this new feature map. The resulting new size is  $317 \times 78$ . Thanks to this size reduction process, time and cost savings are achieved. In addition, results are obtained much faster. The confusion matrix obtained in the proposed method is presented in (Table 7).

The model we proposed obtained the highest accuracy value with an average of 98.94% in the SVM classifier. This was followed by KNN and SE classifiers with 98.34%, respectively. In the proposed model, the lowest average accuracy value was obtained in the DT classifier. The accuracy value obtained in this classifier is 83.92%. Confusion matrices of the three classifiers belonging to the highest mean value obtained in the proposed model are shown in (Table 8).

The suggested approach properly categorized 314 of 317 chest X-ray images while misclassifying three others. The model's total accuracy is 99.05 percent. In the

viral pneumonia class, an image from the suggested model COVID-19 was placed. A perfectly normal image was also incorrectly classified as viral pneumonia. Finally, an image from the viral pneumonia class was placed in the normal class by mistake. With the proposed method, a high level of accuracy was achieved. Deep learning models’ performance can be measured using a variety of indicators. (Table 9) shows the performance metrics achieved using the proposed method.

When (Table 9) is examined, the highest accuracy rate was acquired in the COVID-19 class with 99.27%, while the accuracy value acquired in the Normal and Viral Pneumonia classes was 98.88%.

### The Results Obtained in the Second Data Set with the Proposed Method

The proposed model in this section is tested using a second data set. The accuracy values obtained in the proposed model are given in (Table 10).

Our proposed model achieved the highest accuracy value with an average of 97.1% in the SVM classifier. This was followed by SE classifiers with 96.5% and KNN classifiers with 95.2%, respectively. In the proposed model, the lowest average accuracy value was obtained in the NB classifier. Confusion matrices of the three classifiers with the highest mean value obtained in the proposed model are shown in (Table 11).

**Table 9** Evaluation metrics of the model

	Acc	Sens	Spe	Fpr	Fnr	Fdr	F1
COVID-19	99.27%	100%	99.44%	0.55%	0	0.72%	99.63%
Normal	98.88%	98.88%	99.55%	0.44%	1.11%	0.44%	98.88%
Viral pneumonia	98.88%	97.80%	99.55%	0.44%	2.19%	1.11%	99.33%

**Table 10** Accuracy rates in the second data set of the proposed method

	Accuracy Value of Proposed Models (Mean % ± Standard Deviation)					
	DT	DA	NB	SVM	KNN	SE
Proposed Method	86.1 ± 1.08	96.9 ± 0.73	80.6 ± 1.58	97.1 ± 0.44	95.2 ± 0.96	96.5 ± 0.84

**Table 11** Confusion matrices in the three classifiers, where the model is most successful

	Proposed + SVM			Proposed + KNN			Proposed + SE		
1	687	36		652	69	2	684	36	3
2	19	2012	7	24	1997	17	28	2002	8
3	3	22	244		34	235	2	30	237
	1	2	3	1	2	3	1	2	3

When (Table 11) are examined, it is seen that the highest performance is in the SVM classifier. With the proposed model, it is seen that 2943 of 3030 test images are classified correctly and 87 of them are misclassified in the SVM classifier.

## Discussion

COVID-19 is a deadly serious viral infection that is increasing its prevalence day by day. The disease caused serious damage to public health and the country's economy. The diagnosis of COVID-19 is made by RT-PCR test. However, both the test can be false-negative and the long test results make it difficult for the health services [36]. Therefore, imaging modalities such as chest X-ray and CT have gained importance in the diagnosis phase for better management of the disease [36]. Chest X-ray is increasingly preferred, because it is cheaper than CT, has less radiation exposure and can be transported to different environments [37, 38]. The disease is mainly characterized by pneumonia in the lungs. Pneumonia has many viral and bacterial causes. COVID-19 is just one of them. COVID-19 pneumonia often shows similar chest X-ray findings as other causes of pneumonia [39]. Therefore, it is important to detect COVID-19 pneumonia on chest X-ray images and differentiate it from pneumonia caused by other viruses. Thus, patients can be isolated and treated quickly. In COVID-19 pneumonia, multiple, peripherally located opacities, mainly involving bilateral lower lung lobes, are observed on chest X-rays [39]. In viral pneumonia, bilateral perihilar, peribronchial thickening, and interstitial opacities are seen on chest X-rays, mostly resulting in atelectasis [39]. We diagnosed COVID-19 with a 99.05% success rate with the hybrid model we proposed in our study. Our proposed model predicted 3 images incorrectly. These images are given in (Fig. 3).

Thanks to the proposed artificial intelligence-based model, the diagnosis of COVID-19 disease by experts will take place in a shorter time. Similar studies on the classification of COVID-19 disease in the literature are given in (Table 12).



**Fig. 3** Chest X-ray images that the proposed model predicted incorrectly. **a** This chest X-ray of COVID-19 pneumonia was erroneously classified as viral pneumonia by our model. In the image, the lower lobes of the bilateral lung are normal and the right upper and middle lobes of the right lung are involved, which is not typical for COVID-19 pneumonia. We think that the misclassification is due to this. **b** By our model, a normal chest X-ray was erroneously classified as viral pneumonia. We think that the prominent vascular structures in the image were mistakenly evaluated as opacity. There is no radiological finding compatible with viral pneumonia in the image. **c** A chest X-ray of viral pneumonia was incorrectly classified as normal by our model. However, it is seen that there are interstitial opacities in the bilateral lung, mostly in the lower lobes

**Table 12** Current studies on the classification of COVID-19 chest X-ray images

Study	Year	Models	Performances	Output
Maghdid et al.[9]	2021	Alexnet	94.1%	COVID-19 Normal pneumonia
Yildirim et al.[10]	2020	Hybrit model	96.30%	COVID-19 Normal pneumonia
Asnaoui et al. [11]	2020	Inception-ResnetV2	92.18%	COVID-19 Normal pneumonia
Baltruschat et al.[12]	2019	Resnet38, Resnet50, Resnet101	82.2%	COVID-19 Normal pneumonia
Farid et al. [13]	2020	Future extraction	98.2%	COVID-19 Normal pneumonia
Aslan et al.[14]	2021	CNN, LSTM	98.14%, 98.70%	COVID-19 Normal pneumonia
Khan et al.[15]	2020	Xception	89.6%	COVID-19 Normal pneumonia
Bai et al. [16]	2020	Multilayer perceptions	89.1%	COVID-19 Normal pneumonia
Mahmud et al. [17]	2020	ConvXNet	97.4%	COVID-19 Normal pneumonia
Ucar et al. [18]	2020	SqueezeNet	98.3%	COVID-19 Normal pneumonia
Minae et al. [19]	2020	Transfer Learning	90%	COVID-19 Normal pneumonia
Barua et al. [20]	2021	Hybrid Model	97.60%, 89.96%, 98.84%, 99.64%	COVID-19 Normal pneumonia
Proposed model	–	Hybrid model	99.05%, 97.1%	COVID-19 Normal pneumonia

The main limitation of this study is that it does not provide service over the internet. We are of the opinion that the works that provide services over the internet can be used in different regions.

With the proposed artificial intelligence method, chest X-ray images can be quickly classified and presented to the specialist. Thus, the workload of the specialist will be lightened and the diagnosis of COVID-19 disease will occur in a shorter time.

In the future, it is among our aims to carry out multi-centre and three-dimensional volume-based studies that work over the internet.

## Conclusions

COVID-19 is a fatal disease that can cause acute respiratory distress syndrome, cardiac damage, sepsis, secondary infections, and multi-organ failure. In addition, COVID-19 pneumonia can cause permanent damage to the lungs. Radiologic

methods are used to assist in the diagnosis of COVID-19 and to evaluate the damage it causes to the lungs. However, imaging findings of COVID-19 pneumonia may be confused with other pneumonia. Therefore, we aimed to detect COVID-19 pneumonia in this study and differentiate it from other viral pneumonia causes. In our proposed model, we classified chest X-ray images with an accuracy of 99.05% in the first data set and 97.1% in the second data set. When the obtained accuracy rate is compared with other studies in the literature, it is seen that the proposed model is successful.

**Acknowledgements** We thank the data set owners for sharing their data.

## Declarations

**Conflict of Interest** The authors have not disclosed any conflict of interest.

## References

1. Rothan, H.A., Byrareddy, S.N.: The epidemiology and pathogenesis of coronavirus disease (COVID-19) outbreak. *J. Autoimmun.* **109**, 102433 (2020)
2. Xu, X., et al.: Imaging and clinical features of patients with 2019 novel coronavirus SARS-CoV-2. *Eur. J. Nucl. Med. Mol. Imaging* **47**(5), 1275–1280 (2020). <https://doi.org/10.1007/s00259-020-04735-9>
3. Razai, M.S.: Coronavirus disease 2019 (covid-19): a guide for UK GPs. *Bmj* **368**:m800 (2020)
4. Umakanthan, S., et al.: Origin, transmission, diagnosis and management of coronavirus disease 2019 (COVID-19). *Postgrad. Med. J.* **96**(1142), 753–758 (2020)
5. Pan, F., et al.: Time course of lung changes on chest CT during recovery from 2019 novel coronavirus (COVID-19) pneumonia. *Radiology* **295**, 715–721 (2020)
6. Jacobi, A., et al.: Cardiothoracic imaging portable chest X-ray in coronavirus disease-19 (COVID-19): a pictorial review. *Clinical Imaging* **64**, 35–42 (2020)
7. Jahmunah, V., et al.: Future IoT tools for COVID-19 contact tracing and prediction: a review of the state-of-the-science. *Int. J. Imaging Syst. Technol.* **31**(2), 455–471 (2021)
8. Moitra, D., Mandal, R.K.: Classification of non-small cell lung cancer using one-dimensional convolutional neural network. *Expert Syst. Appl.* **159**, 113564 (2020)
9. Maghdid, H.S., et al.: (2021) Diagnosing COVID-19 pneumonia from X-ray and CT images using deep learning and transfer learning algorithms. In *Multimodal Image Exploitation Learning* **11734**, 117340E (2021). (**International Society for Optics and Photonics**)
10. Yildirim, M., Cinar, A.C.: A deep learning based hybrid approach for COVID-19 disease detections. *Traitement du Signal* **37**(3), 461–468 (2020)
11. El Asnaoui, K., Chawki, Y.: Using X-ray images and deep learning for automated detection of coronavirus disease. *J. Biomol Struct Dyn* **39**, 1–12 (2020)
12. Baltruschat, I.M., et al.: Comparison of deep learning approaches for multi-label chest X-ray classification. *Sci. Rep.* **9**(1), 1–10 (2019)
13. Farid, A.A.: A CNN Classification Model For Diagnosis Covid19 (2020)
14. Aslan, M.F., et al.: CNN-based transfer learning–BiLSTM network: a novel approach for COVID-19 infection detection. *Appl. Soft Comput.* **98**, 106912 (2021)
15. Khan, A.I., Shah, J.L., Bhat, M.M.: CoroNet: A deep neural network for detection and diagnosis of COVID-19 from chest x-ray images. *Comput. Methods Programs Biomed.* **196**, 105581 (2020)
16. Bai, X., et al.: Predicting COVID-19 malignant progression with AI techniques. *SSRN J* (2020). <https://doi.org/10.2139/ssrn.3557984>. (**Preprint posted online on March, 2020, 31**)
17. Mahmud, T., Rahman, M.A., Fattah, S.A.: CovXNet: A multi-dilation convolutional neural network for automatic COVID-19 and other pneumonia detection from chest X-ray images with transferable multi-receptive feature optimization. *Comput. Biol. Med.* **122**, 103869 (2020)

18. Ucar, F., Korkmaz, D.: COVIDiagnosis-Net: deep Bayes-SqueezeNet based diagnosis of the coronavirus disease 2019 (COVID-19) from X-ray images. *Med. Hypotheses* **140**, 109761 (2020)
19. Minaee, S., et al.: Deep-covid: predicting covid-19 from chest x-ray images using deep transfer learning. *Med. Image Anal.* **65**, 101794 (2020)
20. Barua, P.D., et al.: Automatic COVID-19 detection using exemplar hybrid deep features with X-ray images. *Int. J. Environ. Res. Public Health* **18**(15), 8052 (2021)
21. Chowdhury, M.E., et al.: Can AI help in screening viral and COVID-19 pneumonia? *IEEE Access* **8**, 132665–132676 (2020)
22. Rahman, T., et al.: Exploring the effect of image enhancement techniques on COVID-19 detection using chest X-ray images. *Comput. Biol. Med.* **132**, 104319 (2021)
23. Çınar, A., Yıldırım, M., Eroğlu, Y.: Classification of pneumonia cell images using improved ResNet50 model. *Traitement du Signal* **38**(1), 165–173 (2021)
24. Eroglu, Y., Yildirim, M., Cinar, A.: mRMR-based hybrid convolutional neural network model for classification of Alzheimer's disease on brain magnetic resonance images. *Int. J. Imaging Syst. Technol.* **32**(2), 517–527 (2022)
25. Yildirim, M., Cinar, A.: Classification with respect to colon adenocarcinoma and colon benign tissue of colon histopathological images with a new CNN model: MA\_ColonNET. *Int. J. Imaging Syst. Technol.* **32**(1), 155–162 (2022)
26. ZHANG, T., ZHANG, X., SHI, J., WEI, S.: High-speed ship detection in SAR images by improved yolov3. In 2019 16th International Computer Conference on Wavelet Active Media Technology and Information Processing pp. 149–152. IEEE.(2019, December)
27. Howard, A.G., et al.: Mobilenets: efficient convolutional neural networks for mobile vision applications. Preprint [arXiv:1704.04861](https://arxiv.org/abs/1704.04861) (2017)
28. Sandler, M., Howard, A., Zhu, M., Zhmoginov, A., Chen, L. C.: Mobilenetv2: Inverted residuals and linear bottlenecks. In Proceedings of the IEEE conference on computer vision and pattern recognition pp. 4510–4520 (2018)
29. Tan, M., Le, Q.: Efficientnet: Rethinking model scaling for convolutional neural networks. In International conference on machine learning pp. 6105–6114. PMLR. (2019, May)
30. Dogan, S., Akbal, E., Tuncer, T.: A novel ternary and signum kernelled linear hexadecimal pattern and hybrid feature selection based environmental sound classification method. *Measurement* **166**, 108151 (2020)
31. Eroğlu, Y., Yildirim, M., Çınar, A.: Convolutional neural networks based classification of breast ultrasonography images by hybrid method with respect to benign, malignant, and normal using mRMR. *Comput. Biol. Med.* **133**, 104407 (2021)
32. Paoletti, M.E., et al.: A new GPU implementation of support vector machines for fast hyperspectral image classification. *Remote Sensing* **12**(8), 1257 (2020)
33. Koh, J.E.W., et al.: Automated interpretation of biopsy images for the detection of celiac disease using a machine learning approach. *Comput. Methods Programs Biomed.* **203**, 106010 (2021)
34. Cengil, E., Cinar, A.: A deep learning based approach to lung cancer identification. In 2018 International Conference on Artificial Intelligence and Data Processing (IDAP) pp. 1–5. IEEE. (2018, September)
35. Yildirim, M., Çınar, A.: A new model for classification of human movements on videos using convolutional neural networks: MA-Net. *Computer Methods in Biomechanics and Biomedical Engineering: Imaging & Visualization*, **9**(6), 651–659 (2021)
36. Mossa-Basha, M., et al.: Radiology department preparedness for COVID-19: radiology scientific expert review panel. *Radiol Soc North Am* **296**, E106–E112 (2020)
37. Zhao, Y., et al.: Radiology department strategies to protect radiologic technologists against COVID19: experience from Wuhan. *Eur. J. Radiol.* **127**, 108996 (2020)
38. Zanardo, M., Schiaffino, S., Sardanelli, F.: Bringing radiology to patient's home using mobile equipment: a weapon to fight COVID-19 pandemic. *Clin. Imaging* **68**, 99–101 (2020)
39. Cozzi, A., et al.: Chest x-ray in the COVID-19 pandemic: radiologists' real-world reader performance. *Eur. J. Radiol.* **132**, 109272 (2020)